Global Simulation of Land Use/Cover Change Under Shared Socioeconomic Pathways and Impacts On Aboveground Biomass Carbon

Li Zeng[1], Xiaoping Liu[1,2], Wenhao Li[1], Jinpei Ou[1], Yiling Cai[1], Guangzhao Chen[1], Manchun Li[3], Guangdong Li[4], Honghui Zhang[5,6], Xiaocong Xu[1]*

[1]Guangdong Key Laboratory for Urbanization and Geo-simulation, School of Geography and Planning, Sun Yat-sen University, Guangzhou, China.
[2]Southern Marine Science and Engineering Guangdong Laboratory (Zhuhai), Zhuhai, China.
[3]International Institute for Earth System Science, Nanjing University, China.
[4]Key Laboratory of Regional Sustainable Development Modeling, Institute of Geographic Sciences and Natural Resources Research (IGSNRR), Chinese Academy of Sciences (CAS), China.
[5]College of Resources and Environmental Sciences, Hunan Normal University, China.
[6]Guangdong Guodi Planning Science Technology Co., ltd, China.

*Corresponding author: Xiaocong Xu (xuxiaocong@mail.sysu.edu.cn)

Key Points:

- We propose a land use /cover change (LUCC) assessment framework combines the Global Change Assessment Model with the Future Land-Use Simulation model
- We predict the global LUCC at 1-km spatial resolution and 10-year time step from 2010 to 2100, and explore its direct impacts on aboveground biomass carbon (AGB)
- Africa is expected to undergo 58% loss of AGB under scenario SSP3. Aboveground biomass in Asia will fix 3.05 Pg C to reverse the AGB loss in 2100 under scenario SSP1

Abstract

Land use change driven by human activities plays a critical role in terrestrial carbon budget through habitats loss and vegetation change. Despite projections of global population and economic growth under the framework of the shared socioeconomic pathways (SSPs) have been analyzed, little is known about land use /cover change (LUCC) at a fine spatial resolution and how carbon pools respond to LUCC under different SSP scenarios. Here, we projected the future global LUCC at 1-km spatial resolution and 10-year time step from 2010 to 2100, after which its direct impacts on aboveground biomass carbon (AGB) under SSP scenarios were explored. We found that scenario SSP3 yields the highest global cropland expansion, among which about 48% is expected to locate in current forest land and 46% locate in current grassland. Scenario SSP1 has the largest forest expansion, and it is mainly converted from the grassland (54%) and cropland (30%). Due to the spatial change of land use/cover, global AGB loss is expected to reach about 9.16 Pg C in 2100 under scenario SSP3 while increase about 1.75 Pg C under scenario SSP1. Africa is expected to undergo 58% loss of AGB under scenario SSP3. Aboveground biomass in Asia will fix 3.05 Pg C to reverse the AGB loss in 2100 under scenario SSP1. These findings suggest land use development and management is one of key measures to mitigate negative impacts of LUCC on biomass carbon pool.

1 Introduction

Ecosystem service losses driven by land use/cover change (LUCC) are increasing as population and economic growth (Venter et al., 2016; Marques et al., 2019; Ecosystems and human well-being, 2005). As one of key ecosystem services, biomass carbon sequestration is also impacted by LUCC. According to previous research, the terrestrial biosphere has fixing average approximately 2.5 petagrams of carbon per year (Pg C yr^{-1}) which is equal to offset 25% of fossil fuel emissions[4–6]. However, the global net sink in forest land has reduced approximately 1.3 ± 0.7 Pg C yr^{-1} for 1990 to 2007 due to tropical land use change (Pan et al., 2011). The expansion of agricultural area and the change of crop type or agricultural management level lead to the loss of natural vegetation and further results in losses of biomass carbon in local areas (Lawler et al., 2014; van der Hilst et al., 2014; van der Hilst et al., 2018). Biomass carbon includes aboveground biomass carbon (hereinafter referred to as AGB) and belowground biomass carbon (Eggleston, 2006). In this paper, we focus on the AGB as it is directly influenced by LUCC. For both forest and non-forest biomes, over the period 1993–2012, global AGB is estimated to lose average approximately −0.07 Pg C yr^{-1} globally, mostly resulting from the loss of tropical forests (Liu et al., 2015). Over the period 2000–2030, urban expansion will result in 1.38 Pg C (0.05 Pg C yr−1) loss of AGB

within the pan-tropics (Seto et al., 2012). Therefore, it is necessary to estimate the impacts of LUCC on AGB for a better guidance of future carbon management and land use policy development.

To reverse the loss of AGB, the selection of future development pathways, which determine the land use demands, is very important. The shared socioeconomic pathways (SSPs) describe the potential pathways and uncertainties of policy assumptions and the socio-economic storylines based on future global society, population and economic development in the coming century (Riahi et al., 2017; Kriegler et al., 2014). Relative studies on land use demands and LUCC assessment framework under SSPs at a global scale are important but still limited, even though some recent studies have predicted LUCC under SSPs at local-scale (Zhang et al., 2017; Dong et al., 2018). Although global projections of land use demands under SSPs are available, they lack of spatial details for biodiversity assessments (Popp et al., 2017) and climate model projections assessments (Preston et al., 2011). Chen et al. (2020a) estimated the urban land distribution under SSPs, but the other spatially explicit land use types are not included. The Land-Use Harmonization (LUH2) project estimates annually land use fractional patterns for the time period 850-2100 at 0.25° spatial resolution (Hurtt et al., 2020). However, Li et al. has reported that the land use product even at a 10-km resolution is not enough to express sufficient spatial details and may further cause uncertainties in assessing its impacts to environment (Li et al., 2017; Verburg et al., 2006). Therefore, the spatial explicit LUCC at a fine resolution under SSPs are important to manifest the impacts of LUCC on AGB.

Here, we presented global LUCC spatially with a resolution of 1-km under SSPs and explore the direct impacts on AGB. First, the global future land use demands were estimated based on the Global Change Assessment Model (GCAM) with global land use in 2010 and projections of population and economics under SSPs. Then, the Future Land-Use Simulation (FLUS) model was employed to simulate global land use pattern changes at 1-km spatial resolution and 10-year time step from 2010 to 2100 based on land use demands and the driving factors about location and transportation, natural conditions, global land use and social economic. Finally, we estimated the direct impacts of LUCC on AGB with available sources from Liu et al. (2015) under different SSPs.

2 Methods

2.1 The scenario-based LUCC assessment framework

GCAM is an integrated, multisector model reflects the behavior of, and interactions between five systems: energy, agriculture and land use, water, climate, and economy (Shi et al., 2017). Among the global assessment models, GCAM model is able to

express the spatial heterogeneity of land use/cover. Because it can predict the land use/cover demands of 283 world regions, which combine 32 socioeconomic and geopolitical regions with 18 agroecological zones (AEZs) (Calvin et al., 2017; Le Page et al., 2016). It can be coupled to other models for predicting LUCC datasets with greater resolution and reflect the spatial heterogeneity (Cao et al., 2019; Chen et al., 2020b).

In this paper, by integrating GCAM and the LUCC simulation model FLUS, we proposed a scenario-based LUCC assessment framework (GCAM-FLUS) (a detailed flowchart is presented in Figure 1). To accurately estimate the influences of social and economic development on LUCC, first, we input the factors (urbanization rate, population and gross domestic product (GDP) under five SSPs) into GCAM. According to complex socioeconomic assumptions, five systems in GCAM estimate the impacts of global economy and technology on future land use demands. Based on geographic location and income level, GCAM model (http://jgcri.github.io/gcam-doc/overview.html)) aggregates the countries of the world into 32 macro regions (Fig.S1 in Supplemental Material 2). Therefore, the land use demands in different macro regions are obtained from GCAM. Second, through the spatial explicit LUCC model FLUS, the framework realizes the transformation probabilities predictions of land use types and spatial pattern simulation of future LUCC in different macro regions with the quantity constraint of land use demands from GCAM.

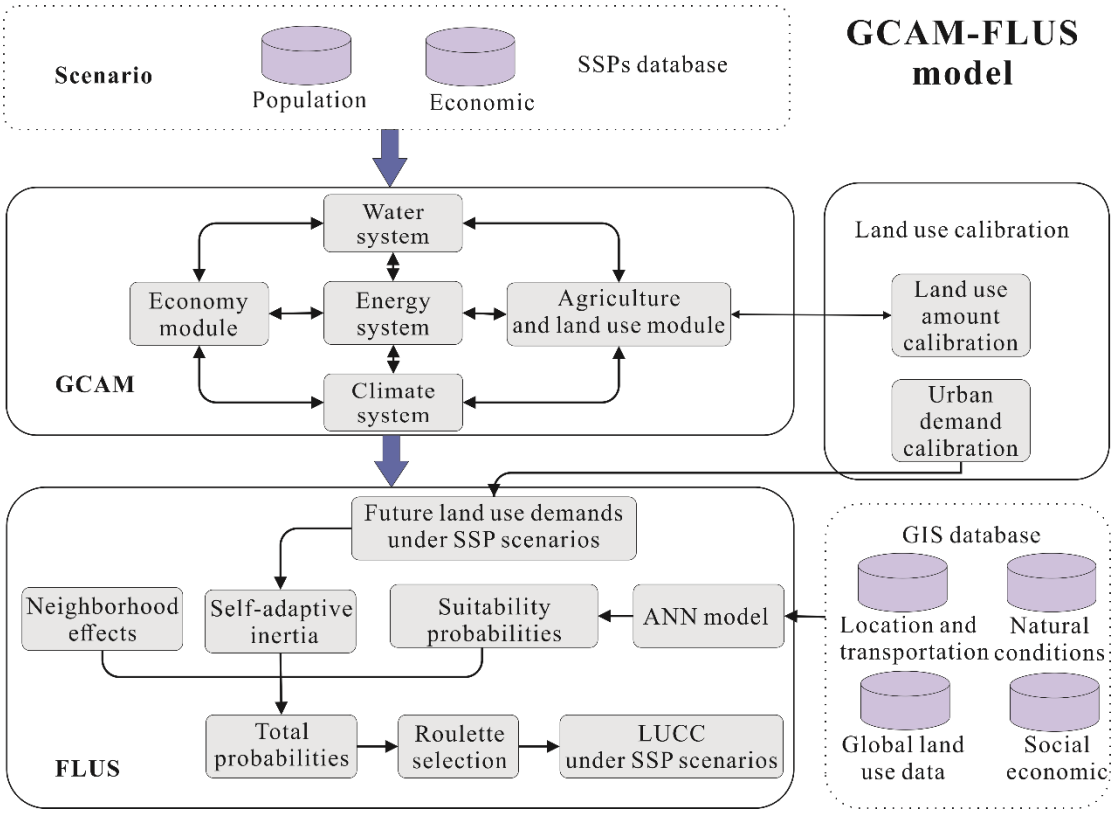

Figure 1. Flowchart of LUCC simulation under SSP scenarios using GCAM-FLUS model.

Specifically, FLUS employs the artificial neural networks (ANNs) to calibrate and

estimate land use suitability probabilities ($sp_{p,k}$) using a set of spatial driving factors (e.g., elevation, slope, population, GDP, distance to city center, distance to roads, soil quality, annual mean temperature, temperature seasonality, annual precipitation, and precipitation seasonality, listed in Table 1) and land use pattern in 2010. Adaptive inertial competition mechanisms and roulette selection mechanisms are designed in FLUS to analyze the influence of the neighborhood land and uncertainty of LUCC (Liu et al., 2017). Adjustment factor ($Inertia_k^t$) is the core content of adaptive inertial competition mechanisms. It is determined according to the difference between the current land use quantity and the land use demand, and adjusted adaptively in the iteration, so that the quantity of each type of land is gradually close to the target quantity in the simulation process:

$$Inertia_k^t = \begin{cases} Inertia_k^{t-1} & \text{if } \left|D_k^{t-2}\right| \le \left|D_k^{t-1}\right| \\ Inertia_k^{t-1} \times \dfrac{D_k^{t-2}}{D_k^{t-1}} & \text{if } 0 > D_k^{t-2} > D_k^{t-1} \\ Inertia_k^{t-1} \times \dfrac{D_k^{t-1}}{D_k^{t-2}} & \text{if } D_k^{t-1} > D_k^{t-2} > 0 \end{cases} \quad (1)$$

where $Inertia_k^t$ is adjustment factor of the land use type k in iteration time t; $D_k^{t\text{-}1}$, $D_k^{t\text{-}2}$ refer to the difference of land use type k between the current and the demand number of pixels in iteration time $t\text{-}1$ and iteration time $t\text{-}2$, respectively.

The land use suitability probabilities ($sp_{p,k}$), neighbourhood effect (Ω) factor, adjustment factor ($inertia_k^t$) and development restriction ($sc_{c\to k}$) are used to calculate total probabilities ($TProb_{p,k}^t$):

$$TProb_{p,k}^t = sp_{p,k} \times \Omega_{p,k}^t \times inertia_k^t \times (1 - sc_{c\to k}) \quad (2)$$

where $TProb_{p,k}^t$ is the total probability that pixel p is transformed into land use type k in iteration time t; $\Omega_{p,k}^t$ is the fraction of existing land use type k in a neighborhood consisting of 5 × 5 grids in iteration time t; $sc_{c\to k}$ refers to the difficulty of transformation.

After the roulette selection, the future spatial pattern of land use in 32 macro regions can be simulated at a 1-km spatial resolution and a 10-year time step from 2020 to 2100 under SSP scenarios. To justify the reliability of the calibrated FLUS model, we

simulated the land use pattern from 2001 to 2010 and compared it to the actual pattern. Figure of Merit (FoM) is employed to assess the model capability for identifying LUCC from 2001 to 2010. The indicator does not have the drawback of overestimation of accuracy like other traditional verification indicators (such as Kappa coefficient) (Pontius et al., 2008; Pontius et al., 2011):

$$FoM = B/(A+B+C+D) \quad (3)$$

where A is the area that is observed change while predicted as unchanged; B is the area that is observed change and also predicted as changed; C denotes the area that is observed change while differs from predicted change; D refers to the area that is observed unchange while predicted as changed.

Table 1

Driving factors for estimating land use suitability probabilities in FLUS

Factors	Name	Year	Resolution	Source
National conditions	DEM	2000	0.5'	Hijmans et al. (2005)
	Slope	2000	0.5'	Retrieved from DEM
	Soil quality (nutrient availability)	2008	5'	Fischer et al. (2008)
	Soil quality (oxygen availability to roots)	2008	5'	
	Soil quality (excess salts)	2008	5'	
	Soil quality (workability)	2008	5'	
	Annual mean temperature	2000	0.5'	Hijmans et al. (2005)
	Annual precipitation	2000	0.5'	
	Temperature seasonality	2000	0.5'	
	Precipitation seasonality	2000	0.5'	
Social economic	GDP	2006	1 km	Ghosh et al. (2010)
	Population	2010	0.5'	Landscan 2010 Global Population Project
Location and transportation	Distance to city center	2014	1 km	United Nations Department of Economic

				and Social Affairs, Population Division (2014)
	Distance to roads	1980-2010	1 km	NASA, Socioeconomic Data and Applications Center, Global Roads Open Access Data Set, version 1

176

177 2.2 Calibration of initial land amounts for GCAM and estimation of future urban land

178 demands

179 In the GCAM, historical land use data are from FAO/GTAP (2010; 2006), SAGE
180 (Ramankutty and Foley, 1999), and HYDE (Goldewijk, 2001), and they are classified
181 into 10 types, including urban land, forest, shrub, rock, pasture, grassland, tundra,
182 desert, ice, and biomass (Kyle et al., 2011). To guarantee data consistency over the land
183 use simulation framework, we used the MODIS Land Cover Type Product (Friedl et al.,
184 2010) (MCD12Q1; https://lpdaac.usgs.gov/) in 2010 to calibrate the land use types in
185 GCAM, including eliminate the inconsistencies between those two land use
186 classification schemes and the discrepancies of land amounts. First, the land use data
187 are reclassified into six types in harmony with two datasets (see Table 2). Detailed crop
188 types in GCAM are unified to cropland. Managed and unmanaged pasture, protected
189 grassland and grassland are reclassified into Grassland. Second, we calibrate the initial
190 land use data using MCD12Q1 data to establish a series of new GCAM land use inputs.
191 Based on the unification of classification in Table 1, the land amounts in 2010 of
192 MODIS data are divided to initial land amounts of detailed types according to the
193 original proportion of each type in GCAM.
194 As a constraint condition, the land use demands estimated by GCAM help to simulate
195 the spatial distribution of future LUCC and further investigate potential impacts on
196 global ecosytem and environment. However, the future urban land demands always
197 remain unchanged in GCAM (Kyle et al., 2011), therefore, calibration should be carried
198 out accordingly before the land use spatially allocation. Here, the future urban land
199 demands are derived from the results in our previous study (Chen et al., 2020a), which
200 adopted the panel data regression to calculate future urban land demands.
201 **Table 2**
202 *Reclassification for land use types among GCAM, MODIS and FLUS model in this*
203 *research*

GCAM land types	MODIS	FLUS land types
Crop	Cropland/natural vegetation	Cropland

Other arable land	mosaics	
Biomass		
Managed/unmanaged forest	Evergreen needleleaf forests	Forest
	Evergreen broadleaf forests	
	Deciduous needleleaf forests	
	Deciduous broadleaf forests	
	Mixed forests	
Protected shrub/shrub	Closed shrublands	
	Open shrublands	
Managed/unmanaged pasture	Woody savannas	Grassland
Protected grassland/grassland	Savannas	
	Grasslands	
Urban land	Urban and built-up lands	Urban
Tundra, ice, rock, desert	Snow and ice	Barren
	Barren or sparsely vegetated	
None	Water bodies	Water
	Permanent wetlands	

2.3 Impacts of LUCC on AGB

In this study, the InVEST (Integrated Valuation of Ecosystem Services and Tradeoffs) model was used to estimate the impacts of LUCC on AGB. InVEST model was jointly designed, developed and maintained by three organizations: the Nature Conservancy, Stanford University and the World Wide Fund for Nature. It aims to simulate the changes in the quantity and value of ecosystems services under different land use scenarios. The Carbon module in the InVEST model directly estimates the impacts of LUCC on the carbon storage (including AGB, belowground biomass carbon, soil organic carbon and litter carbon) of terrestrial ecosystems based on carbon density and land use. Here, the method is introduced to estimate the impacts of LUCC on AGB. First, we employ the overlay analysis among the Global Ecological Zone map (GEZ, available at: http://foris.fao.org/static/data/fra2010/ecozones2010.jpg), AGB in 2010 (Liu et al., 2015) and land use in 2010 to calculate the average carbon density of each land use type in different climate zones. Then, LUCC datasets between 2010 and each SSP scenario are multiplied by carbon density, respectively (see in fomula (4)). Finally, the loss of AGB due to LUCC under five SSPs scenarios are estimated in each continent every 10 years from 2010 to 2100:

$$\Delta C_{t1 \to t2} = \sum_{i=1,k=1}^{m,n} C_{ik,t} / N_{ik,t} \times (N_{ik,t2} - N_{ik,t1}) \quad (4)$$

where $\Delta C_{t1 \to t2}$ denotes the loss of AGB between $t2$ and $t1$; $C_{ik,t}$ is the known

total AGB of land use type k in ecozone i when time t; $N_{ik,t}$, $N_{ik,t1}$ and $N_{ik,t2}$ refers to the pixels' number of land use type k in ecozone i when time t, $t1$ and $t2$, respectively.

3 Results

3.1 Projection of future land use area demands

Our results show that there are distinctive differences of the global land use demands among the five SSP scenarios (Figure 2). Turning points of land use demands are observed during the 2060s and 2080s, after which urban and cropland demands are expected to decline while forest and grassland demands are rising. The cropland demand is increased by about 30% in 2100 compared with 2010 under scenario SSP3. For the other scenarios, the demands for cropland are likely to rise before 2070s and then fall. It shows a significant downward trend and the smallest forest demand (4.4×10^7 km^2) under scenario SSP3, while scenario SSP2 yields the smallest grassland demand (3.6×10^7 km^2). The urban demands under scenarios SSP2, SSP3, and SSP5 show monotonically increasing trends, among which scenario SSP5 is the most distinctive one with almost twice urban area demand (1.3×10^6 km^2) by the end of this century compared with that in 2010 (6.7×10^5 km^2).

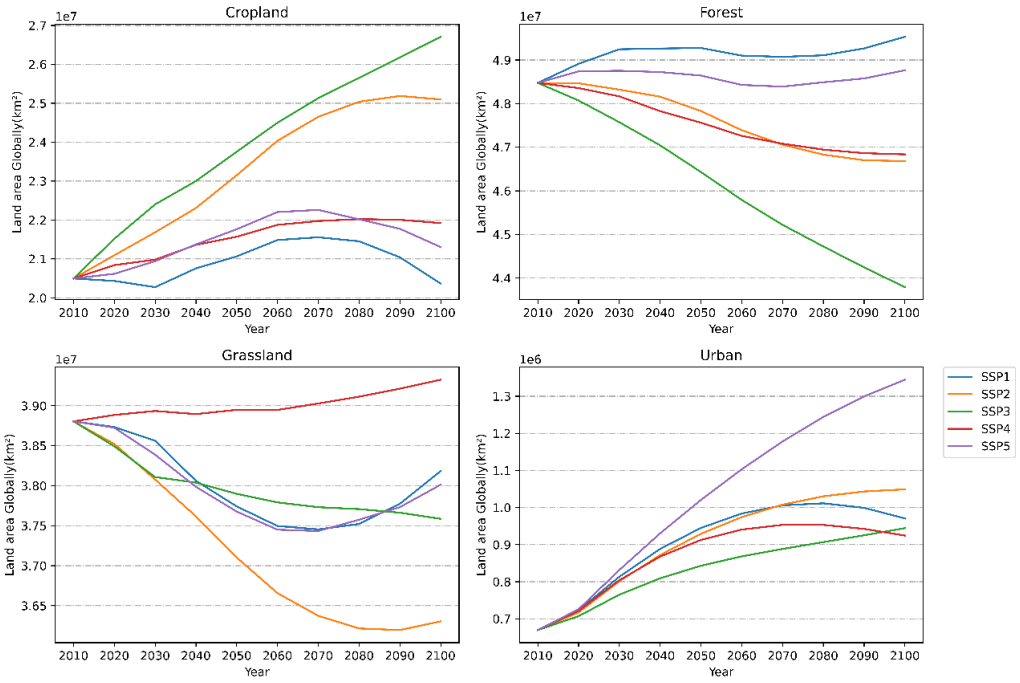

Figure 2. Projections of land use demands globally for 2010–2100 under SSP scenarios.

We also found large gap of the land use demands among different regions worldwide. Three representative regions, namely China, the USA and Brazil, are selected to show

their distinctive development paths for 2010–2100 (Fig.S2-S4 in Supplemental Material 2) , respectively. In China, unlike the global and the other two regions, the demand for forest land shows an upward trend and highly reach 2.3×10^6 km^2 under scenario SSP1 by the end of the century, while urban demand shows a trend of first growth and then decline, with the turning point in the 2040s or 2050s. In the USA, the trend of LUCC under each scenario is roughly similar to that of the world. In Brazil, it is notable that the continual growth of urban demand and the largest demand (3.9×10^4 km^2) area are found under scenario SSP3. Scenario SSP3 also yields the dramatic decline of grassland demand and the smallest demand area (3.5×10^6 km^2).

3.2 Global LUCC simulations during 2010 - 2100

To highlight the change of land use between 2010 and 2100, we employ focal summation statistics on the results of the simulated LUCC maps with a radius of 15 km. Figure 3 shows the transition of cropland area in 2100 under scenarios SSP3 and SSP5 in the selected representative regions of China, the USA and Brazil. Results show that these three regions experience more cropland expansion under scenario SSP3 than that in SSP5. One potential reason maybe that scenario SSP3 is a regional development trajectory and has a higher population increasement and larger amount of food demand.

Maps of global LUCC (including cropland, forest, grassland and urban) for each SSP scenario are shown in Fig.S5-S8 (Supplemental Material 2), respectively. The detailed information about simulated LUCC between 2010 and 2100 under each SSP are shown in Fig.S9 (Supplemental Material 2) and statistical analysis for the results within continental regions are listed in Table S1 (Supplemental Material 1). We find that scenario SSP3 yields the highest global cropland expansion. Cropland expansion area mainly distribute in Africa, increased by 33.5%-68.7% in 2100 compared with 2010. The global forest land area decreases the most under scenario SSP3 while increase under scenario SSP1. The decrease of forest land in Africa is very obvious, ranging from -6.5% (SSP1) to -38.6% (SSP3) in 2100 compared with 2010. However, forest land in Asia and Europe under scenario SSP1 has increased by 5.4% and 6.5%, respectively. The area of grassland has reduced the most under scenario SSP2. The grassland area in Africa has a large change which ranges from -14.2% under scenario SSP2 to 7.9% under scenario SSP3. The global urban area has expanded the most under scenario SSP5. Among them, North America has the largest expansion area at 272,651 km^2, and the largest expansion intensity is in Oceania, which is an increase of 178.3% compared with 2010.

In addition to the spatiotemporal pattern of LUCC, the transfer between land use types is also very important to assess the AGB budget. In order to facilitate the following assessment of the impact of LUCC on AGB, we draw a pixel map to describe land use transfer. Each pixel represents the maximum area of land use transfer that may occur during 2010-2100 and its corresponding area (Figure 4). In the vertical direction, we can find that scenario SSP3 will occur the largest cropland expansion, and the

expansion is mainly due to the occupation of the current forest (48%) and grassland (46%). Scenario SSP1 has the largest expansion of forest, and it is mainly from the current grassland (54%), followed by cropland (30%). Scenario SSP5 yields the largest urban expansion and 60% of the expansion was due to the occupation of cropland. In the horizontal direction, we can find that the degradation of forest is more obvious under scenario SSP3, and most of them degenerate into cropland and grassland.

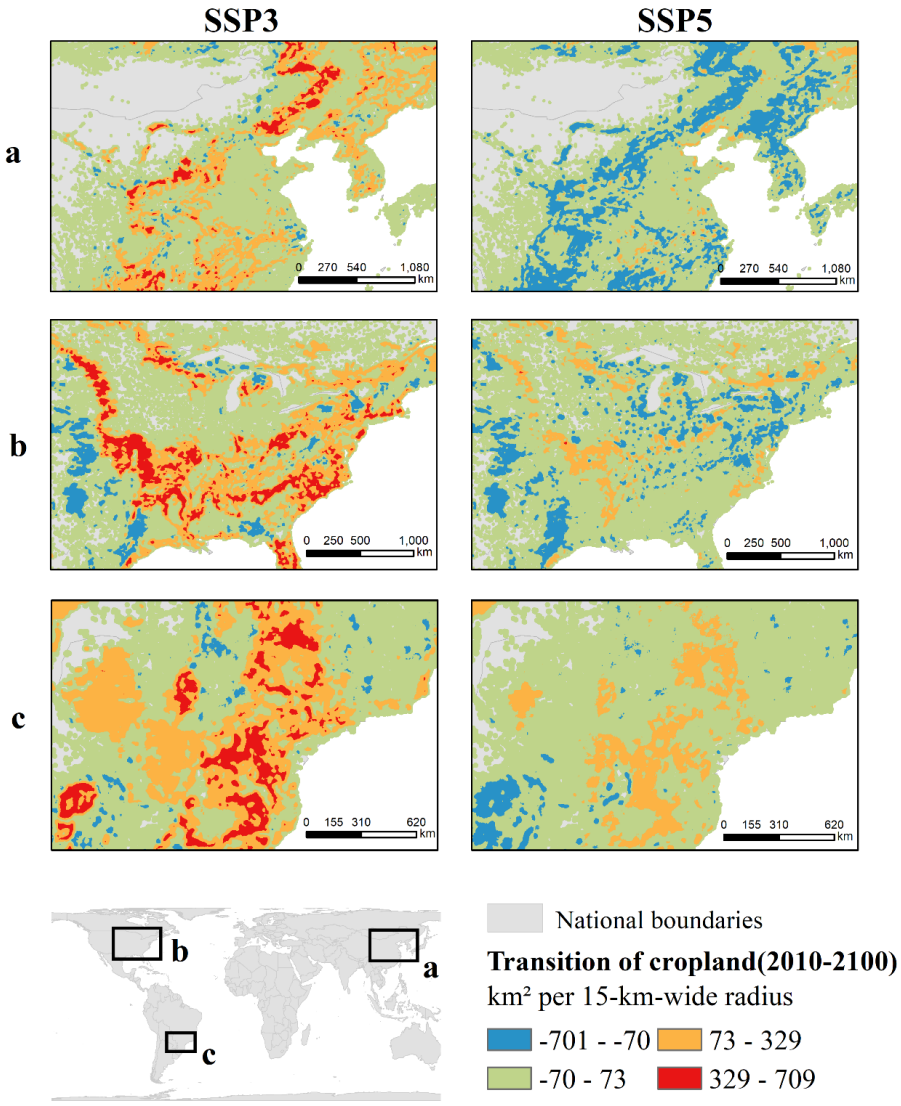

Figure 3. Global projections of cropland transition between 2010 and 2100 under scenario SSP3 and SSP5 in representative regions. a China, b the USA, c Brazil. We adopt focal statistics to deal with the simulated maps for better visualization. The results show that these three regions experience more cropland expansion under scenario SSP3 than in SSP5. Cropland area in China are dramatically decrease in SSP5.

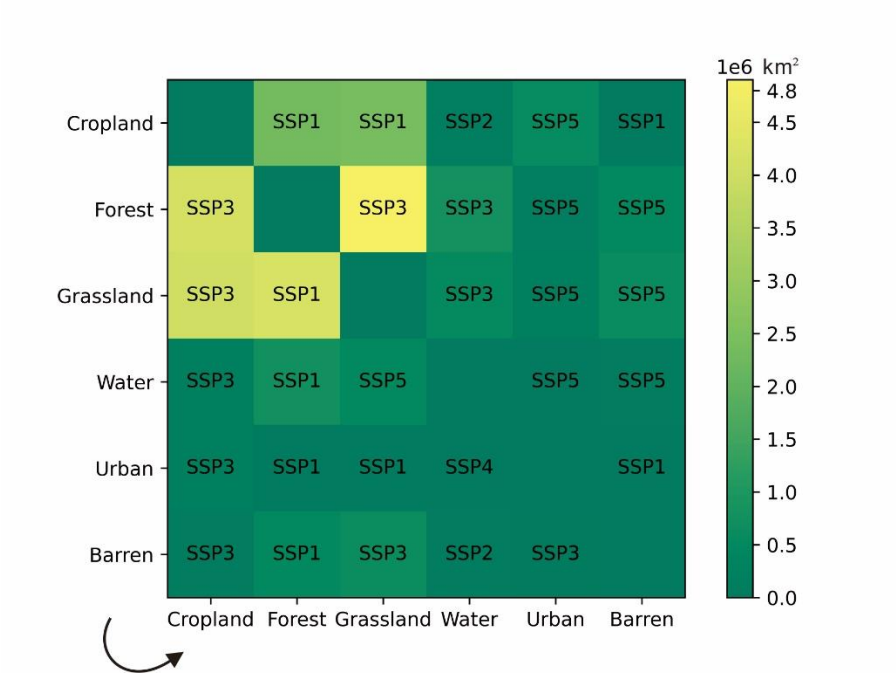

Figure 4. The maximum area and its interrelated scenario of land use conversion during 2010 – 2100 under SSP scenarios.

We adopted FoM to quantitatively evaluate the performance of FLUS simulation model. The range of FoM is between 0 and 1. The higher value means less differences between the simulation and the observed change. By comparing our simulation land use patterns with MCD12Q1 land use product in 2010, we estimated the FoM indicator in 32 macro regions (Table 3). The values of FoM in 32 macro regions range from 12% to 37% and their average value is 22%, which is similar to or even higher than other land use simulation studies. For example, Liu et al. (2017) has simulated multiple LUCC between 2000 and 2010 in China and the FoM is 19.62 percent. Li et al. (2017) reported their values of FoM in global 17 regions are about 10- 29 percent. It means the model has good fit between the simulation and the observed change and has enough accuracy to simulate future LUCC.

Table 3

The values of Figure of Merit of the GCAM regions for global land use simulation from 2001 to 2010

Region	Abbreviation	FoM (%)	Region	Abbreviation	FoM (%)
Africa_Eastern	EAF	24.2	European Free Trade Association	EFTA	26.6
Africa_Northern	NAF	23.6	India	INDI	27.5
Africa_Southern	RSAF	16.2	Indonesia	INDO	12.2
Africa_Western	WAF	29.8	Japan	JAP	12.2
Argentina	ARG	12.7	Mexico	MEX	23.6
Australia_NZ	ANZ	30.3	Middle East	ME	24.6

Brazil	BRA	30.9	Pakistan	PAKI	29.6
Canada	CAN	13.6	Russia	RUS	13.6
Central America and Caribbean	CAC	17.9	South Africa	SAF	28.7
Central Asia	CTA	36.8	South America_Northern	SAN	11.9
China	CHN	26.3	South America_Southern	SAS	23.2
Colombia	CLM	23.4	South Asia	SA	26.1
EU-12	EU-12	18.1	South Korea	KOR	31.7
EU-15	EU-15	15.0	Southeast Asia	SEA	18.6
Europe_Eastern	EURE	21.1	USA	USA	21.8
Europe_Non_EU	EURN	20.5			

Note. Region names follow the definition of GCAM4 model region in documentation for GCAM (http://jgcri.github.io/gcam-doc/overview.html).

Different from other land use products with coarse resolution, the resolution of our products is 1 km, which can reflect more details of LUCC. In order to intuitively compare the spatial differences of land use products with different resolutions, we resampled land use in 2050 under scenario SSP1 to 10km based on the majority values of the original land use in 10 km^2-grid. Comparing the land use patterns of three representative regions: Pearl River Delta in China, California in the United States and Rio de Janeiro in Brazil (Figure 5), it can be found that the 1-km resolution image can better express the real distribution of cities, while the 10-km resolution image has obvious patch effects. This is owing to the scattered pixels around the city are classified as other land and the final urban area of 10-km resolution will less than that of 1-km resolution.

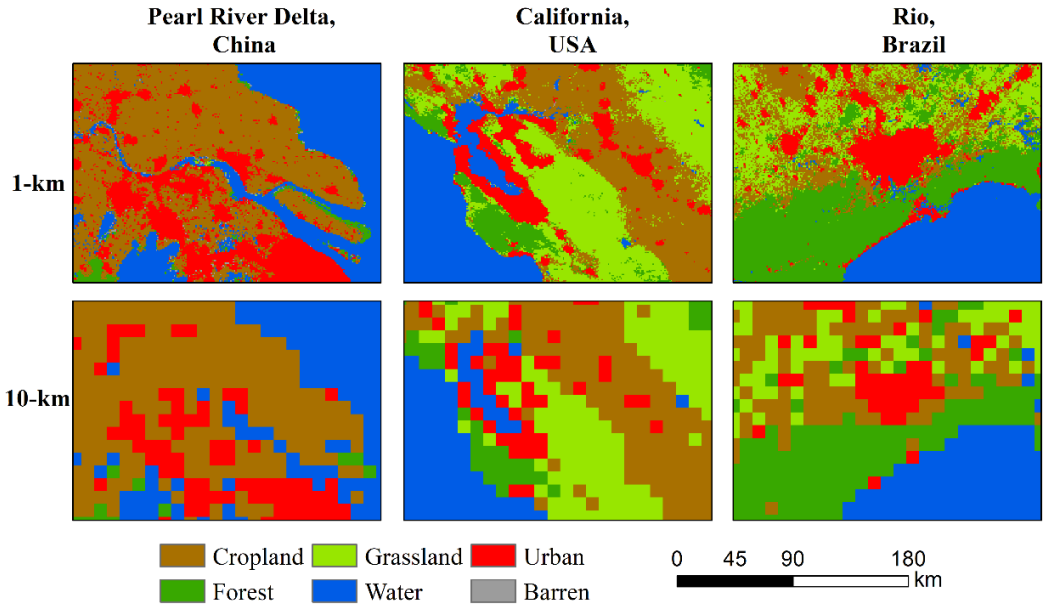

Figure 5. The spatial differences between land use products with 1-km and 10-km resolution in three representative regions.

3.3 Spatial-explicit AGB loss driven by LUCC

Based on average carbon density of each land use type in different climate zones (see Methods), the loss of AGB due to LUCC under five SSPs scenarios are mapped in Figure 6. We find the loss are mainly located in central Africa where is around Congo Rainforest (approximately 4.58 Pg C loss from 2010 to 2100 under scenario SSP3), which is consistent with results in Liu et al (Liu et al., 2015) . The changes of AGB within continents over the period 2010-2100 for the SSP scenarios are shown in Table 4. The greatest losses of AGB are most likely in Africa, with estimates from 1.22 Pg C (SSP1) to 5.35Pg C (SSP3) across five SSP scenarios. This may be due to the substantial forest land losses which hava a higher carbon density (Table S1 in Supplemental Material 1). North America and South America are also suffered, particularly under scenario SSP3, losing about 1.73 Pg C and 1.41 Pg C, respectively. What stands out in the table is the high growth of AGB in Asia, which has increases of 1.55-3.05Pg C except under scenario SSP3. According to the simulated LUCC in Asia, we find that the AGB increase in Asia may be related to the expansion of forest in this area. Under scenario SSP3, the forest area in Asia loses 8.49×10^5 km^2 in 2100 compared with 2010, far more than that under scenario SSP2 (5.83×10^4 km^2), while it increases under scenarios SSP1, SSP4 and SSP5, highly reaching 8.61×10^5 km^2 (SSP1) at most (Table S1 in Supplemental Material 1). We further estimated the global change of AGB over the period of 2010-2100 across five SSP scenarios. The global AGB increases by 1.75 Pg C and 0.79 Pg C under scenario SSP1 and scenario SSP5, respectively, while decreases in the rest three scenarios, among which AGB loss under scenario SSP3 is the most significant, reaching 9.16Pg C by the end of the century.

Table 4

The change of aboveground biomass carbon (Pg C) within continents and the whole world over the period 2010 to 2100 under SSP scenarios

Scenario	Continents						Global
	Africa	Asia	Europe	North America	Oceania	South America	
SSP1	-1.22	3.05	0.30	-0.73	-0.02	0.37	1.75
SSP2	-2.32	1.55	-0.50	-1.36	0.06	-0.67	-3.24
SSP3	-5.35	-0.47	-0.38	-1.73	0.18	-1.41	-9.16
SSP4	-4.70	2.20	0.32	-0.93	0.08	0.05	-2.99
SSP5	-1.20	2.72	0.20	-0.98	0.00	0.04	0.79

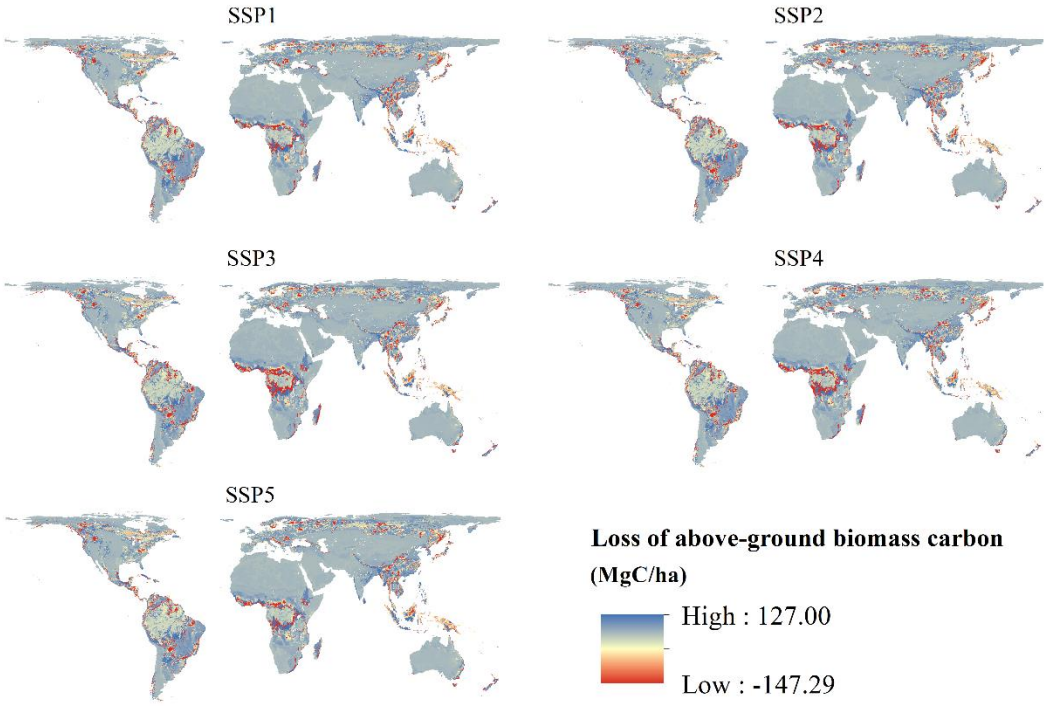

Figure 6. Spatial explicit change of AGB caused by LUCC over the period 2010 to 2100 across SSP scenarios.

In addition to the large-scale statistics of AGB change under SSP scenarios in the future, we discuss the importance of high-resolution land use products on the fine spatial assessment of future AGB for regional scale. Taking central Africa as an example, we compare the land use pattern and the corresponding AGB changes between 2010 and 2100 under scenario SSP1 and SSP3 (Figure 7). We find the high-value regions of AGB change mainly locate in area where grassland converts to cropland. The low-value regions of AGB change mainly occurred in area where forest coverts to cropland and to grassland. LUCC from 2010 to 2100 in central Africa are highlighted by cropland growth and forest degradation. The density of AGB of forest and cropland in central Africa are higher than other land use types. As a result, the change of AGB in this area is mainly due to the location of cropland growth and forest degradation.

The spatial difference between scenario SSP1 and SSP3 mainly locates around the Congo Basin. Under scenario SSP1, grassland is replaced by cropland, while under scenario SSP3, forest is replaced by cropland and grassland. Therefore, the loss of AGB under scenario SSP3 is larger than that under scenario SSP1.

In the change evaluation of AGB for different scenarios, the resolution of land use products is very important. Because the grids of 1×1 km may contain different ages of forests, and their respective carbon density are also different. High-resolution land use provides the possibility to identify the specific degradation location of forest and its impact on AGB change.

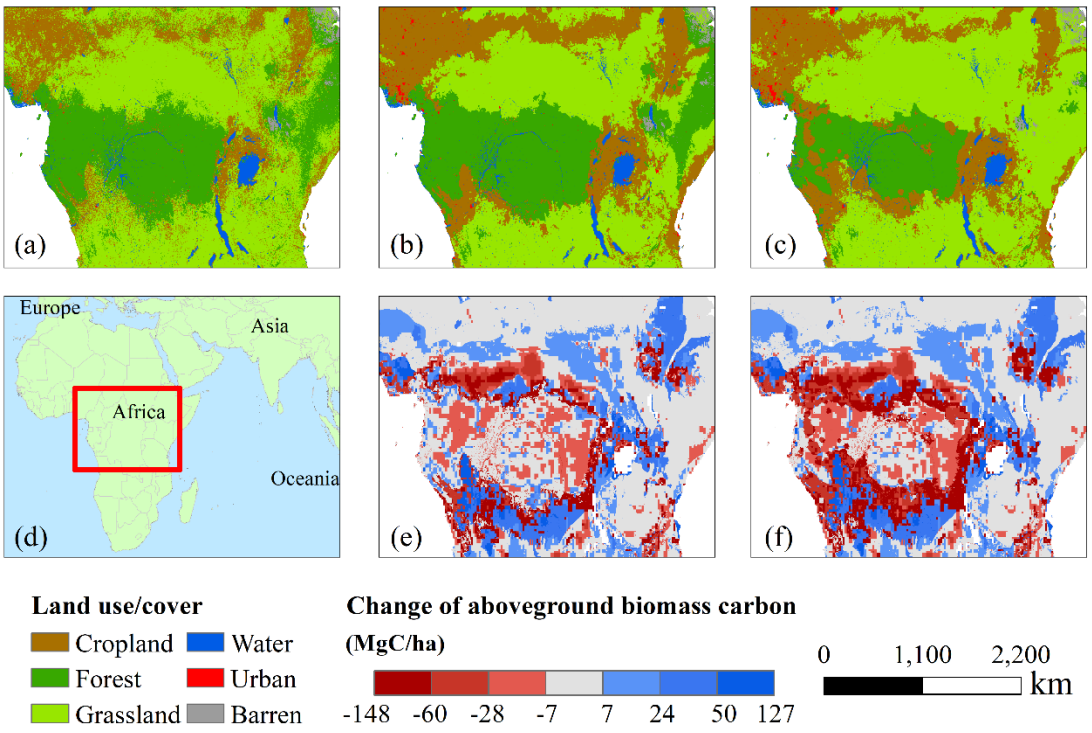

Figure 7. Land use/cover in 2010 (a) and in 2100 under scenario SSP1 (b) and scenario SSP3 (c) in central Africa. Spatial explicit change of AGB caused by LUCC over the period 2010 to 2100 under scenario SSP1 (e) and SSP3 (f).

4 Discussion

In this paper, we proposed a GCAM-FLUS model to simulate future LUCC with a fine spatial resolution of 1 km for the latest SSP scenarios. The uncertainties of model include stochastic uncertainty, heterogeneity and structural uncertainty (Briggs et al., 2012). To quantify the stochastic uncertainty, we adopted kernel density analysis with 5-km-radius to evaluate the likelihood of land to become cropland, forest, grassland and urban land. Taking the results of SSP2 scenario in 2100 as an example, Figure 8 shows that each land use type has a high likelihood with its main patches while a lower likelihood at the edge of patches. It suggests that the spatial stochastic uncertainties exist but stable and acceptable. To solve heterogeneity uncertainty, we predicted the land use demand and simulated the long-term spatial pattern of LUCC within different macro regions separately (follow the definition of GCAM model region (http://jgcri.github.io/gcam-doc/overview.html)). To estimate structural uncertainty of our model, we compared our land use products with Min Chen's work (Chen et al., 2020b) in GCAM4 model regions (Figure 9). It provides a new global gridded land use dataset for 2015–2100 at 0.05° resolution using GCAM and Demeter (Vernon et al., 2018) (a land use spatial downscaling model), under SSP scenarios and Representative

Concentration Pathway (RCP) scenarios. We find that the cropland area simulated by our model in GCAM4 model regions have a high consistency with Chen's results by a significant Pearson correlation coefficient of 0.95. The consistency is also high with forest area between our results and Chen's results (Pearson correlation coefficient is 0.92). The Pearson correlation coefficient of grassland area, barren area and water area are 0.84, 0.88 and 0.87, respectively.

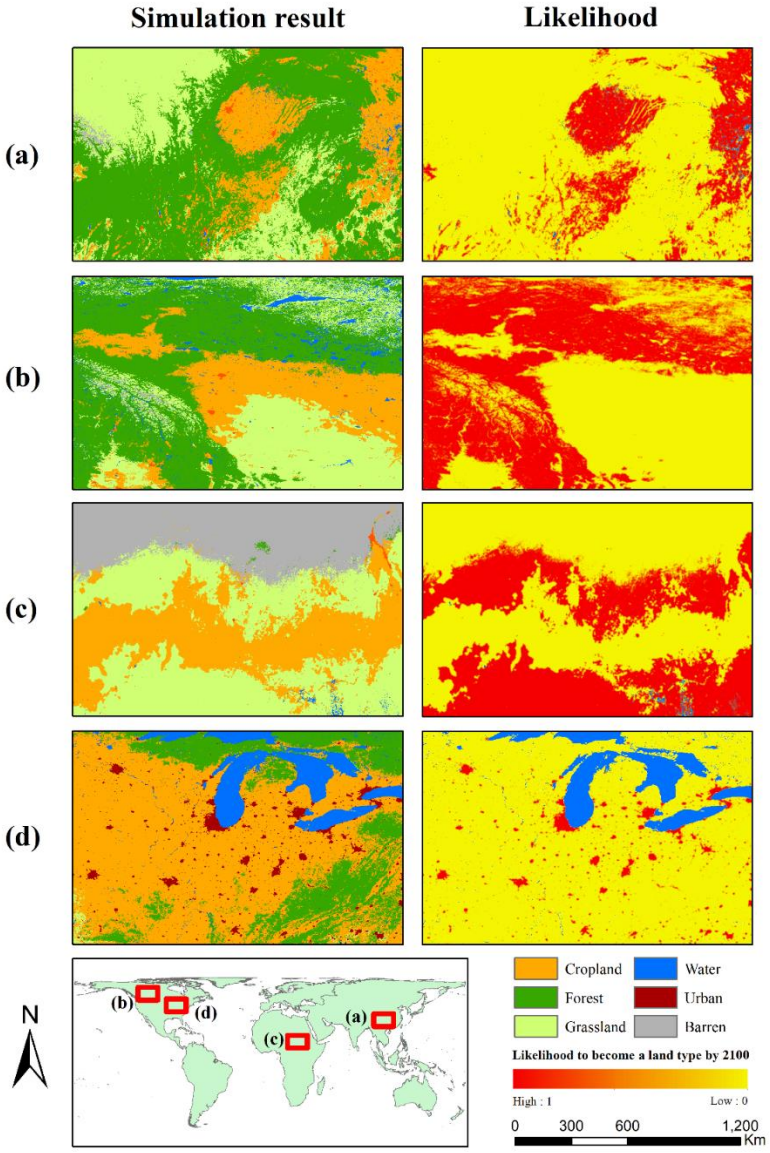

Figure 8. Uncertainty in the simulation results of (a)cropland, (b)forest, (c)grassland and (d)urban in the SSP2 scenario in 2100.

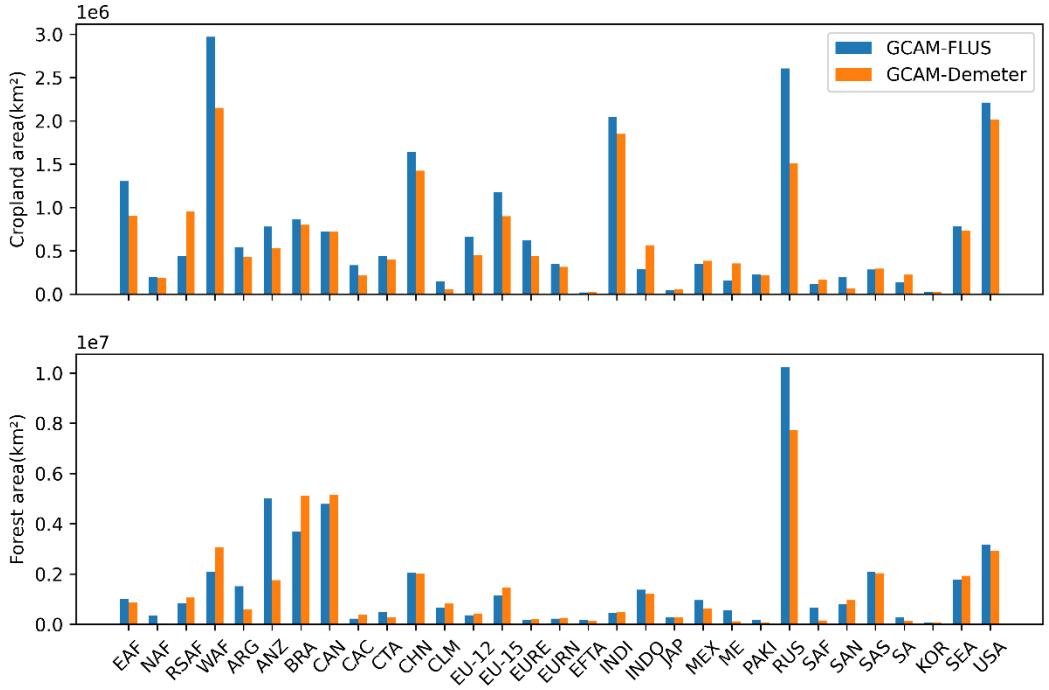

Figure 9. Comparison of cropland area (top) and forest area (bottom) of 2050 in different regions simulated by Chen's GCAM-Demeter model and our GCAM-FLUS model.

In InVEST model, the carbon density of a land use type is equal to the average of the whole carbon pools of the land use type in unit area, which keeps static during the study period. In other words, each land use type is assigned with a fixed and unique carbon density value. It makes the InVEST model stable and is suitable for estimating the change of AGB impacted by LUCC. However, at the same time, it also results in difficulties of capturing small changes of AGB for the same land use type. For example, felling old forests or young forests, resulting in different losses of AGB and the former loses more than the latter. In the future research, we will try to subdivide the forest by vegetation function type and tree age, so as to capture the changes of AGB during forest felling and restoration. Another shortcoming of InVEST model is that it ignores the process of carbon flow between AGB pool and other carbon pools. When forest is replaced by barren land, the trunk may be taken away for use or become dead wood and the residues such as branches and leaves will be transferred to the dead organic carbon pool. However, this part of carbon is considered to lose from pools and emission to the atmosphere in the model. As a result, the carbon emissions caused by LUCC may be overestimated.

Except the uncertainties of models, there are several other limitations. First, spatial driving factors keep unchanged for all SSP scenarios and are same with in 2010. Because it's hard to acquire the reliable predictions of future urban infrastructure. Second, we don't calibrate the errors of misclassification in history land use products and it may be retained into our final results. Third, the impacts of climate to LUCC are

not considered in this research. We may take it account in future work by incorporating RCP scenarios with SSP scenarios.

5 Conclusions

The change of land use caused by human activities is not only a local issue, but also has significant impacts on global biomass carbon. In this paper, we presented the long-term land use pattern predictions with a finer spatial resolution (1 km) under SSP scenarios. High-resolution LUCC helps us to identify the specific spatial location of land use types interrelated with high carbon density and evaluate its impact on AGB change accurately. We find the global AGB increases by 1.75 Pg C and 0.79 Pg C under scenario SSP1 and scenario SSP5, respectively, while decreases in the rest three scenarios, particularly under scenario SSP3, reaching 9.16Pg C by the end of the century. The losses of AGB are mainly located in central Africa where is around Congo Rainforest with estimates of 5.35Pg C under scenario SSP3. This may be due to the loss of substantial forest land with a higher carbon density. On the contrary, AGB in Asia occurs a high growth of 3.05Pg C under scenario SSP1. Therefore, LUCC under scenario SSP1 gives a better development example to alleviate AGB loss which is focus on forest restoration and protection under a green and sustainable pathway. Moreover, the LUCC dataset is based on the latest SSP scenarios under CMIP6, which lay the base for research in other associated disciplines, such as ecological assessment (Li et al., 2020), biodiversity protection (Jantz et al., 2015), global environmental change analyses (Thuiller et al., 2008) and sustainable development planning (Nobre et al., 2016).

Code availability

We used the FLUS software for generating modelling results in this manuscript. FLUS is freely accessible to all users can be downloaded at http://www.geosimulation.cn/flus.html.

Acknowledgements

This study was supported by the National Key Research and Development Program of China (grants 2017YFA0604404 and 2019YFA0607203), the National Natural Science Foundation of China (grants 41801304, 41901327 and 42001326), the Fundamental Research Funds for the Central Universities (grants 19lgpy41 and 19lgpy53), the project funded by China Postdoctoral Science Foundation

(2020T130732)

References

Briggs, A., Weinstein, M., Fenwick, E., Karnon, J., Sculpher, M.& Paltiel, A. (2012). Model parameter estimation and uncertainty: a report of the ISPOR-SMDM Modeling Good Research Practices Task Force--6. *Value in health: the journal of the International Society for Pharmacoeconomics and Outcomes Research, 15* (6), 835–842. https://doi.org/10.1016/j.jval.2012.04.014

Calvin, K., Wise, M., Kyle, P., CLARKE, L.& EDMONDS, J. (2017). A hindcast experiment using the GCAM 3.0 agriculture and land-use module. *Climate Change Economics, 08* (01), 1750005. https://doi.org/10.1142/S2010007817500051

Cao, M., Zhu, Y., Quan, J., Zhou, S., Lü, G., Chen, M.& Huang, M. (2019). Spatial sequential modeling and predication of global land use and land cover changes by integrating a global change assessment model and cellular automata. *Earth's Future, 7* (9), 1102–1116. https://doi.org/10.1029/2019EF001228

Chen, G., Li, X., Liu, X., Chen, Y., Liang, X., Leng, J. et al. (2020a). Global projections of future urban land expansion under shared socioeconomic pathways. *Nature communications, 11* (1), 537. https://doi.org/10.1038/s41467-020-14386-x

Chen, M., Vernon, C., Graham, N., Hejazi, M., Huang, M., Cheng, Y.& Calvin, K. (2020b). Global land use for 2015-2100 at 0.05° resolution under diverse socioeconomic and climate scenarios. *Scientific data, 7* (1), 320. https://doi.org/10.1038/s41597-020-00669-x

Dong, N., You, L., Cai, W., Li, G.& Lin, H. (2018). Land use projections in China under global socioeconomic and emission scenarios: Utilizing a scenario-based land-use change assessment framework. *Global Environmental Change, 50*, 164–177. https://doi.org/10.1016/j.gloenvcha.2018.04.001

Ecosystems and human well-being (2005). Washington, DC: World Resources Institute

Eggleston, H. S. (Ed.) (2006). 2006 IPCC guidelines for national greenhouse gas inventories. Volume 4 Agriculture, forestry and other land use. International Panel on Climate Change, 2006. Hayama, Japan: Institute for Global Environmental Strategies. Available online at https://www.ipcc-nggip.iges.or.jp/public/2006gl/pdf/4_Volume4/V4_01_Ch1_Introduction.pdf

FAO (2006). Global Forest Resources Assessment 2005

FAO (2010). Global Forest Resources Assessment

Fischer, G., F. Nachtergaele, S. Prieler, H. T.van Velthuizen, L. Verelst, and D. Wiberg. (Ed.) (2008). Global agro-ecological zones assessment for agriculture (GAEZ 2008). Laxenburg, Austria, and Rome, Italy: IIASA and FAO

Friedl, M., Sulla-Menashe, D., Tan, B., Schneider, A., Ramankutty, N., Sibley, A.& Huang, X. (2010). MODIS Collection 5 global land cover: Algorithm refinements and characterization of new datasets. *Remote Sensing of Environment, 114* (1), 168–

182. https://doi.org/10.1016/j.rse.2009.08.016

Goldewijk, K. (2001). Estimating global land use change over the past 300 years: The HYDE Database. *Global Biogeochemical Cycles, 15* (2), 417–433. https://doi.org/10.1029/1999GB001232

Hijmans, R., Cameron, S., Parra, J., Jones, P.& Jarvis, A. (2005). Very high resolution interpolated climate surfaces for global land areas. *International Journal of Climatology, 25* (15), 1965–1978. https://doi.org/10.1002/joc.1276

Hurtt, G., Chini, L., Sahajpal, R., Frolking, S., Bodirsky, B., Calvin, K. et al. (2020). Harmonization of global land use change and management for the period 850–2100 (LUH2) for CMIP6. *Geoscientific Model Development, 13* (11), 5425–5464. https://doi.org/10.5194/gmd-13-5425-2020

Jantz, S., Barker, B., Brooks, T., Chini, L., Huang, Q., Moore, R. et al. (2015). Future habitat loss and extinctions driven by land-use change in biodiversity hotspots under four scenarios of climate-change mitigation. *Conservation Biology, 29* (4), 1122–1131. https://doi.org/10.1111/cobi.12549

Kriegler, E., Edmonds, J., Hallegatte, S., Ebi, K., Kram, T., Riahi, K. et al. (2014). A new scenario framework for climate change research: the concept of shared climate policy assumptions. *Climatic Change, 122* (3), 401–414. https://doi.org/10.1007/s10584-013-0971-5

Kyle, G., Luckow, P., Calvin, K., Emanuel, W., Nathan, M.& Zhou, Y. (2011). GCAM 3.0 Agriculture and Land Use: Data Sources and Methods. Pacific Northwest National Laboratory (PNNL). Richland, Washington

Lawler, J., Lewis, D., Nelson, E., Plantinga, A., Polasky, S., Withey, J. et al. (2014). Projected land-use change impacts on ecosystem services in the United States. *Proceedings of the National Academy of Sciences, 111* (20), 7492–7497. https://doi.org/10.1073/pnas.1405557111

Lazar, M. (2010). Shedding light on the global distribution of economic activity. *The Open Geography Journal, 3* (1), 147–160. https://doi.org/10.2174/1874923201003010147

Le Page, Y., West, T., Link, R.& Patel, P. (2016). Downscaling land use and land cover from the Global Change Assessment Model for coupling with Earth system models. *Geoscientific Model Development, 9* (9), 3055–3069. https://doi.org/10.5194/gmd-9-3055-2016

Li, H., Zhao, Y.& Zheng, F. (2020). The framework of an agricultural land-use decision support system based on ecological environmental constraints. *The Science of the total environment, 717*, 137149. https://doi.org/10.1016/j.scitotenv.2020.137149

Li, X., Chen, G., Liu, X., Liang, X., Wang, S., Chen, Y. et al. (2017). A new global land-use and land-cover change product at a 1-km resolution for 2010 to 2100 based on human–environment interactions. *Annals of the American Association of Geographers, 107* (5), 1040–1059. https://doi.org/10.1080/24694452.2017.1303357

Liu, X., Liang, X., Li, X., Xu, X., Ou, J., Chen, Y. et al. (2017). A future land use simulation model (FLUS) for simulating multiple land use scenarios by coupling

549 human and natural effects. *Landscape and Urban Planning, 168*, 94–116.
550 https://doi.org/10.1016/j.landurbplan.2017.09.019
551 Liu, Y., van Dijk, A., Jeu, R. de, Canadell, J., McCabe, M., Evans, J.& Wang, G. (2015).
552 Recent reversal in loss of global terrestrial biomass. *Nature Climate Change, 5* (5),
553 470–474. https://doi.org/10.1038/nclimate2581
554 Marques, A., Martins, I., Kastner, T., Plutzar, C., Theurl, M., Eisenmenger, N. et al.
555 (2019). Increasing impacts of land use on biodiversity and carbon sequestration
556 driven by population and economic growth. *Nature ecology & evolution, 3* (4), 628–
557 637. https://doi.org/10.1038/s41559-019-0824-3
558 Nobre, C., Sampaio, G., Borma, L., Castilla-Rubio, J., Silva, J.& Cardoso, M. (2016).
559 Land-use and climate change risks in the Amazon and the need of a novel sustainable
560 development paradigm. *Proceedings of the National Academy of Sciences, 113* (39),
561 10759–10768. https://doi.org/10.1073/pnas.1605516113
562 Pan, Y., Birdsey, R., Fang, J., Houghton, R., Kauppi, P., Kurz, W. et al. (2011). A large
563 and persistent carbon sink in the world's forests. *Science (New York, N.Y.), 333*
564 (6045), 988–993. https://doi.org/10.1126/science.1201609
565 Pontius, R., Boersma, W., Castella, J.-C., Clarke, K., Nijs, T. de, Dietzel, C. et al.
566 (2008). Comparing the input, output, and validation maps for several models of land
567 change. *The Annals of Regional Science, 42* (1), 11–37.
568 https://doi.org/10.1007/s00168-007-0138-2
569 Pontius, R., Peethambaram, S.& Castella, J.-C. (2011). Comparison of three maps at
570 multiple resolutions: A case study of land change simulation in Cho Don District,
571 Vietnam. *Annals of the Association of American Geographers, 101* (1), 45–62.
572 https://doi.org/10.1080/00045608.2010.517742
573 Popp, A., Calvin, K., Fujimori, S., Havlik, P., Humpenöder, F., Stehfest, E. et al. (2017).
574 Land-use futures in the shared socio-economic pathways. *Global Environmental*
575 *Change, 42*, 331–345. https://doi.org/10.1016/j.gloenvcha.2016.10.002
576 Preston, B., Yuen, E.& Westaway, R. (2011). Putting vulnerability to climate change on
577 the map: a review of approaches, benefits, and risks. *Sustainability Science, 6* (2),
578 177–202. https://doi.org/10.1007/s11625-011-0129-1
579 Ramankutty, N.& Foley, J. (1999). Estimating historical changes in global land cover:
580 Croplands from 1700 to 1992. *Global Biogeochemical Cycles, 13* (4), 997–1027.
581 https://doi.org/10.1029/1999GB900046
582 Riahi, K., van Vuuren, D., Kriegler, E., Edmonds, J., O'Neill, B., Fujimori, S. et al.
583 (2017). The Shared Socioeconomic Pathways and their energy, land use, and
584 greenhouse gas emissions implications: An overview. *Global Environmental Change,*
585 *42*, 153–168. https://doi.org/10.1016/j.gloenvcha.2016.05.009
586 Seto, K., Güneralp, B.& Hutyra, L. (2012). Global forecasts of urban expansion to 2030
587 and direct impacts on biodiversity and carbon pools. *Proceedings of the National*
588 *Academy of Sciences of the United States of America, 109* (40), 16083–16088.
589 https://doi.org/10.1073/pnas.1211658109
590 Shi, W., Ou, Y., Smith, S., Ledna, C., Nolte, C.& Loughlin, D. (2017). Projecting

state-level air pollutant emissions using an integrated assessment model: GCAM-USA. *Applied energy, 208*, 511–521. https://doi.org/10.1016/j.apenergy.2017.09.122

Thuiller, W., Albert, C., Araújo, M., Berry, P., Cabeza, M., Guisan, A. et al. (2008). Predicting global change impacts on plant species' distributions: Future challenges. *Perspectives in Plant Ecology, Evolution and Systematics, 9* (3-4), 137–152. https://doi.org/10.1016/j.ppees.2007.09.004

van der Hilst, F., Verstegen, J., Woltjer, G., Smeets, E.& Faaij, A. (2018). Mapping land use changes resulting from biofuel production and the effect of mitigation measures. *GCB Bioenergy, 10* (11), 804–824. https://doi.org/10.1111/gcbb.12534

van der Hilst, F., Verstegen, J., Zheliezna, T., Drozdova, O.& Faaij, A. (2014). Integrated spatiotemporal modelling of bioenergy production potentials, agricultural land use, and related GHG balances; demonstrated for Ukraine. *Biofuels, Bioproducts and Biorefining, 8* (3), 391–411. https://doi.org/10.1002/bbb.1471

Venter, O., Sanderson, E., Magrach, A., Allan, J., Beher, J., Jones, K. et al. (2016). Sixteen years of change in the global terrestrial human footprint and implications for biodiversity conservation. *Nature communications, 7*, 12558. https://doi.org/10.1038/ncomms12558

Verburg, P., Schulp, C.J.E., Witte, N.& Veldkamp, A. (2006). Downscaling of land use change scenarios to assess the dynamics of European landscapes. *Agriculture, Ecosystems & Environment, 114* (1), 39–56. https://doi.org/10.1016/j.agee.2005.11.024

Vernon, C., Le Page, Y., Chen, M., Huang, M., Calvin, K., Kraucunas, I.& Braun, C. (2018). Demeter – A land use and land cover change disaggregation model. *Journal of Open Research Software, 6* (4), 311. https://doi.org/10.5334/jors.208

Zhang, D., Huang, Q., He, C.& Wu, J. (2017). Impacts of urban expansion on ecosystem services in the Beijing-Tianjin-Hebei urban agglomeration, China: A scenario analysis based on the Shared Socioeconomic Pathways. *Resources, Conservation and Recycling, 125*, 115–130. https://doi.org/10.1016/j.resconrec.2017.06.003

Competing interests

The authors declare no competing interests

Supplementary data

Supplementary material related to this article can be found in the Supplemental Material 1.docx and Supplemental Material 2.docx.